Peroxisomal Hydrogen Peroxide Is Coupled to Biotic Defense Responses by ISOCHORISMATE SYNTHASE1 in a Daylength-Related Manner[1][C][W][OA]

Sejir Chaouch, Guillaume Queval[2], Sandy Vanderauwera, Amna Mhamdi, Michaël Vandorpe, Mathilde Langlois-Meurinne, Frank Van Breusegem, Patrick Saindrenan, and Graham Noctor*

Institut de Biologie des Plantes, UMR8618 CNRS, Université de Paris Sud, 91405 Orsay cedex, France (S.C., G.Q., A.M., M.L.-M., P.S., G.N.); Department of Plant Systems Biology, Flanders Institute for Biotechnology, 9052 Ghent, Belgium (S.V., M.V., F.V.B.); and Department of Plant Biotechnology and Genetics, Ghent University, 9052 Ghent, Belgium (S.V., M.V., F.V.B.)

While it is well established that reactive oxygen species can induce cell death, intracellularly generated oxidative stress does not induce lesions in the Arabidopsis (*Arabidopsis thaliana*) photorespiratory mutant *cat2* when plants are grown in short days (SD). One interpretation of this observation is that a function necessary to couple peroxisomal hydrogen peroxide (H_2O_2)-triggered oxidative stress to cell death is only operative in long days (LD). Like lesion formation, pathogenesis-related genes and camalexin were only induced in *cat2* in LD, despite less severe intracellular redox perturbation compared with SD. Lesion formation triggered by peroxisomal H_2O_2 was modified by introducing secondary mutations into the *cat2* background and was completely absent in *cat2 sid2* double mutants, in which ISOCHORISMATE SYNTHASE1 (ICS1) activity is defective. In addition to H_2O_2-induced salicylic acid (SA) accumulation, the *sid2* mutation in ICS1 abolished a range of LD-dependent pathogen responses in *cat2*, while supplementation of *cat2* with SA in SD activated these responses. Nontargeted transcript and metabolite profiling identified clusters of genes and small molecules associated with the daylength-dependent ICS1-mediated relay of H_2O_2 signaling. The effect of oxidative stress in *cat2* on resistance to biotic challenge was dependent on both growth daylength and ICS1. We conclude that (1) lesions induced by intracellular oxidative stress originating in the peroxisomes can be genetically reverted; (2) the isochorismate pathway of SA synthesis couples intracellular oxidative stress to cell death and associated disease resistance responses; and (3) camalexin accumulation was strictly dependent on the simultaneous presence of both H_2O_2 and SA signals.

Reactive oxygen species (ROS) are major players in stress conditions and in developmental signaling (Mittler et al., 2004; Gapper and Dolan, 2006). Among the best studied processes involving ROS are biotic interactions, notably responses to pathogens during which ROS production has been implicated in various defense processes, such as cell death initiation, as well as phytoalexin production and systemic acquired resistance (Dietrich et al., 1994; Lamb and Dixon, 1997; Torres et al., 2006; Van Breusegem and Dat, 2006).

Most of the focus on pathogen-triggered ROS production has concerned apoplastic production by NADPH oxidases or peroxidases (Torres et al., 2005; Bindschedler et al., 2006; Sagi and Fluhr, 2006; Vlot et al., 2009). However, ROS can be produced at high rates in several intracellular compartments, especially chloroplasts, mitochondria, and peroxisomes (Foyer and Noctor, 2003), and it is widely assumed that "oxidative damage" is a major consequence of increased ROS availability in these organelles (del Río et al., 2006; Møller et al., 2007; Nishizawa et al., 2008; Triantaphylidès et al., 2008).

Outstanding questions are the roles of different ROS and different compartments in ROS production. Recent data indicate that chloroplast-linked oxidative stress is mainly attributable to singlet oxygen rather than hydrogen peroxide (H_2O_2; Triantaphylidès et al., 2008), while modeling showed that the chloroplast electron transport chain would have to devote a very high proportion of electrons to oxygen in order to meet the high rates of photorespiratory H_2O_2 production in the peroxisomes (Noctor et al., 2002; Foyer and Noctor,

[1] This work was supported by the Centre National de la Recherche Scientifique (Ph.D. fellowship to S.C.), the French Agence Nationale de la Recherche-GENOPLANTE (grant no. GNP0508G to P.S. and G.N.), the Scientific Exchange Program Flanders-France (grant no. Tournesol T.2008.21 to F.V.B. and G.N.), and the Research Foundation-Flanders (postdoctoral fellowship to S.V.).

[2] Present address: Department of Plant Systems Biology, Flanders Institute for Biotechnology, and Department of Plant Biotechnology and Genetics, Ghent University, 9052 Ghent, Belgium.

* Corresponding author; e-mail graham.noctor@u-psud.fr.

The author responsible for distribution of materials integral to the findings presented in this article in accordance with the policy described in the Instructions for Authors (www.plantphysiol.org) is: Graham Noctor (graham.noctor@u-psud.fr).

[C] Some figures in this article are displayed in color online but in black and white in the print edition.

[W] The online version of this article contains Web-only data.

[OA] Open Access articles can be viewed online without a subscription.

www.plantphysiol.org/cgi/doi/10.1104/pp.110.153957

2003). Peroxisomal H_2O_2 is notably metabolized by catalases, although ascorbate peroxidases are also associated with peroxisomes (del Río et al., 2006; Narendra et al., 2006; Nyathi and Baker, 2006). Catalase-deficient lines have been particularly useful in the analysis of oxidative stress responses (Takahashi et al., 1997; Willekens et al., 1997; Chamnongpol et al., 1998; Mittler et al., 1999; Rizhsky et al., 2002; Dat et al., 2003; Vandenabeele et al., 2004; Vanderauwera et al., 2005; Queval et al., 2007). Under conditions where photorespiratory H_2O_2 production is highly active, catalase-deficient barley (*Hordeum vulgare*), tobacco (*Nicotiana tabacum*), and Arabidopsis (*Arabidopsis thaliana*) lines have all been shown to display a marked perturbation of intracellular redox state, measured as glutathione status (Smith et al., 1984; Willekens et al., 1997; Queval et al., 2007). In tobacco, such redox perturbation has been linked to the activation of certain pathogen-associated processes such as lesion formation, salicylic acid (SA) accumulation, and induction of pathogenesis-related (*PR*) genes (Takahashi et al., 1997; Chamnongpol et al., 1998; Mittler et al., 1999). Crossing with *nahG* lines that express a bacterial SA hydroxylase diminished some of these effects but did not reverse lesion formation (Takahashi et al., 1997).

Cell death induced by chloroplastic overproduction of singlet oxygen can be largely prevented by secondary "executor" mutations (Wagner et al., 2004). Whereas high light-induced lesions in catalase-deficient tobacco could be blocked pharmacologically (Dat et al., 2003), no study has yet reported the genetic reversion of cell death triggered specifically by intracellular H_2O_2. Previously, we reported that responses to H_2O_2-induced oxidative stress in the Arabidopsis *cat2* knockout mutant were highly determined by growth daylength (Queval et al., 2007). Whereas marked intracellular redox perturbation was evident in both short days (SD) and long days (LD), lesion formation was specific to LD conditions. This daylength dependence of oxidative stress responses could be explained in two ways. First, lesions could appear in LD but not in SD because longer exposure to intracellular H_2O_2 causes antioxidative defense withdrawal. Second, the effect of daylength would reflect an executor-type function in LD that is absent or less active in SD. If cell death in LD is mediated through an execution pathway, it should be possible to genetically uncouple intracellular H_2O_2-triggered oxidative stress from lesion formation.

Here, we report that increased peroxisomal availability of H_2O_2 in *cat2* triggers pathogen defense responses and resistance in a strictly daylength-dependent manner that is independent of the degree of intracellular redox perturbation. We further show that peroxisomal H_2O_2-induced lesions can be completely reverted by blocking SA synthesis and provide evidence that the reversion does not occur either through defense withdrawal or by decreasing the degree of intracellular oxidative stress. Finally, we use the daylength dependence of the *cat2* mutant to identify defense-related metabolites that are under the control of H_2O_2, SA, or both.

RESULTS

LD-Specific Activation of Pathogen Response in *cat2*

To investigate the interaction between daylength and intracellular H_2O_2 in pathogen responses, *PR1* transcripts were quantified in ecotype Columbia (Col-0) and *cat2* at a standard irradiance of 200 μmol m^{-2} s^{-1} in LD (16 h of light/8 h of dark) and compared with levels in SD (8 h of light/16 h of dark) at a 2-fold higher irradiance. This analysis showed that *PR1* was much more strongly induced in *cat2* grown in LD (Fig. 1A). Even at lower irradiance (100 μmol m^{-2} s^{-1}), *PR1* transcripts were 3-fold higher in LD than in SD at a 4-fold higher irradiance (data not shown). Thus, *PR1* expression was induced by H_2O_2 in a daylength-dependent manner that is independent of the light dose. Daylength-dependent effects were thereafter analyzed at a constant moderate irradiance of 200 μmol m^{-2} s^{-1}.

Both SA and the phytoalexin camalexin were significantly accumulated only in *cat2* plants in LD (Fig. 1, B, C, and F). A similar response was found for the coumarin scopoletin, which is also increased during biotic interactions (Chong et al., 2002). Like both free and glucosylated forms of SA, scopoletin accumulated strongly in *cat2* in LD but remained at wild-type levels in SD (Fig. 1).

To further explore whether lesions in *cat2* in LD are related to known pathogen signaling pathways, the mutant was crossed with loss-of-function mutants of the cell death regulators *LSD1* and *bZIP10* (Dietrich et al., 1994; Kaminaka et al., 2006). In SD, no lesions in any of the genotypes were apparent (data not shown). In LD, neither *lsd1* nor *bzip10* single mutants displayed visible cell death, whereas approximately 13% of the *cat2* rosette presented spreading lesions (Fig. 2, A and B). Compared with *cat2*, lesions appeared earlier in *cat2 lsd1* and later in *cat2 bzip10*. After 21 d of growth, both double mutants showed significantly different percentage lesion areas compared with *cat2*, with more widespread cell death in *cat2 lsd1* and less cell death in *cat2 bzip10* (Fig. 2B). All *cat2* genotypes showed higher SA contents than Col-0, *lsd1*, and *bzip10* (Fig. 2, C and D).

Genetic Reversion of Cell Death in *cat2*

Because the *cat2* mutation triggers SA accumulation in conditions permissive for cell death, we crossed this mutant with the *sid2-1* mutant (Supplemental Fig. S1), which is defective in ISOCHORISMATE SYNTHASE1 (ICS1). This enzyme is essential in the production of SA in Arabidopsis plants exposed to pathogens (Wildermuth et al., 2001), and hence blocking its activity is more pathway-specific than the use of *nahG* expression, which may also lead to interference from

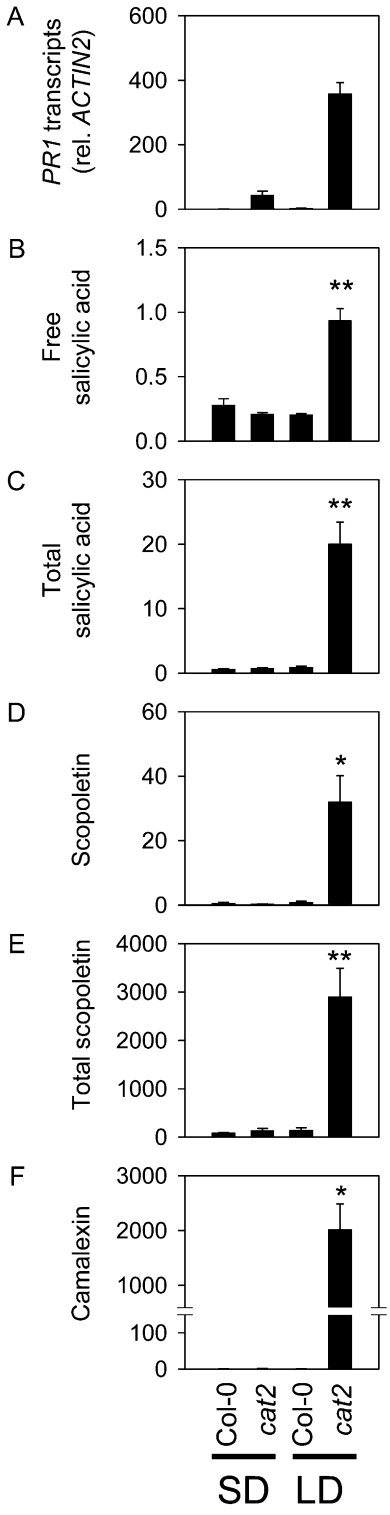

Figure 1. Induction of defense transcripts, SA, and phytoalexins is dependent on LD in *cat2*. A, *PR1* transcripts, relative to *ACTIN2* transcripts. B, Free SA (μg g^{-1} fresh weight). C, Total SA (free + SA glucoside; μg g^{-1} fresh weight). D, Scopoletin (ng g^{-1} fresh weight). E, Total scopoletin (free + glucoside; ng g^{-1} fresh weight). F, Camalexin (ng g^{-1} fresh weight). Data are means ± SE of three independent leaf extracts taken from different plants. Significant differences between Col-0 and *cat2* in each condition are indicated as follows: * $P < 0.05$, ** $P < 0.01$.

elevated levels of SA metabolites such as catechol (Van Wees and Glazebrook, 2003). Whereas SA accumulation in *cat2* in LD exceeded 20 times the levels in Col-0 (Fig. 1), total SA contents, quantified as μg g^{-1} fresh weight in *cat2 sid2* (0.23 ± 0.01), were very similar to those observed in *sid2* (0.23 ± 0.005); that is, 20% to 30% of the basal levels observed in the wild type (0.92 ± 0.17). Blocking SA synthesis through this pathway in *cat2 sid2* reverted the peroxisomal H_2O_2-induced cell death phenotype of *cat2* in LD but did not affect the *cat2*-decreased growth phenotype in SD (Fig. 3, A–C). When grown at high CO_2 to suppress photorespiratory H_2O_2 production and oxidative stress in *cat2* (Queval et al., 2007, 2009) all four genotypes developed similarly and no decrease in growth was observed relative to the wild type (Supplemental Fig. S2).

Various issues may render H_2O_2 assays imprecise (Queval et al., 2008). Using the sensitive luminol luminescence technique, no difference was detected in leaf extracts from any of the genotypes in either growth condition (Fig. 3D). This observation is in agreement with previous studies of catalase-deficient tobacco and barley lines. It may indicate that peroxisomal H_2O_2 does not make a major contribution to overall tissue contents of peroxides or that other antioxidative systems replace catalase in *cat2*. Engagement of other H_2O_2-metabolizing systems in catalase-deficient plants is evidenced by adjustments in intracellular redox state at the level of the glutathione pool (Willekens et al., 1997; Noctor et al., 2002; Rizhsky et al., 2002). Therefore, we quantified reduced and oxidized forms of glutathione as a sensitive indicator of intracellular redox status. The *sid2* mutant showed similar glutathione status to Col-0, whereas in *cat2*, glutathione contents were significantly increased, notably due to accumulated oxidized glutathione levels (Fig. 3E). Glutathione was less perturbed in *cat2* in LD than in SD, and in both conditions it was at least as perturbed in *cat2 sid2* as in *cat2*. In SD, glutathione status in *cat2 sid2* and *cat2* was similar (Fig. 3E, right), in agreement with the lack of effect of the *sid2* mutation on the *cat2* phenotype in this condition (Fig. 3, A and C). In LD, however, the glutathione pool was more oxidized in *cat2 sid2* than in *cat2* (Fig. 3E, left). Thus, as well as reverting LD-dependent lesion formation in *cat2*, blocking the isochorismate pathway of SA synthesis also shifted glutathione status toward that observed in SD.

Interactions between Peroxisomal H_2O_2 and SA in the Modulation of Metabolite Profiles

Nontargeted metabolite profiling by gas chromatography (GC)-time of flight-mass spectrometry (MS) was performed on Col-0, *sid2*, *cat2*, and *cat2 sid2* plants grown in either SD or LD. This analysis identified 106 unique compounds. Metabolites showing significant intersample variation (ANOVA, $P < 0.05$) were identified and subsequently subjected to hierarchical clustering (Fig. 4A). This analysis revealed (1) that many of

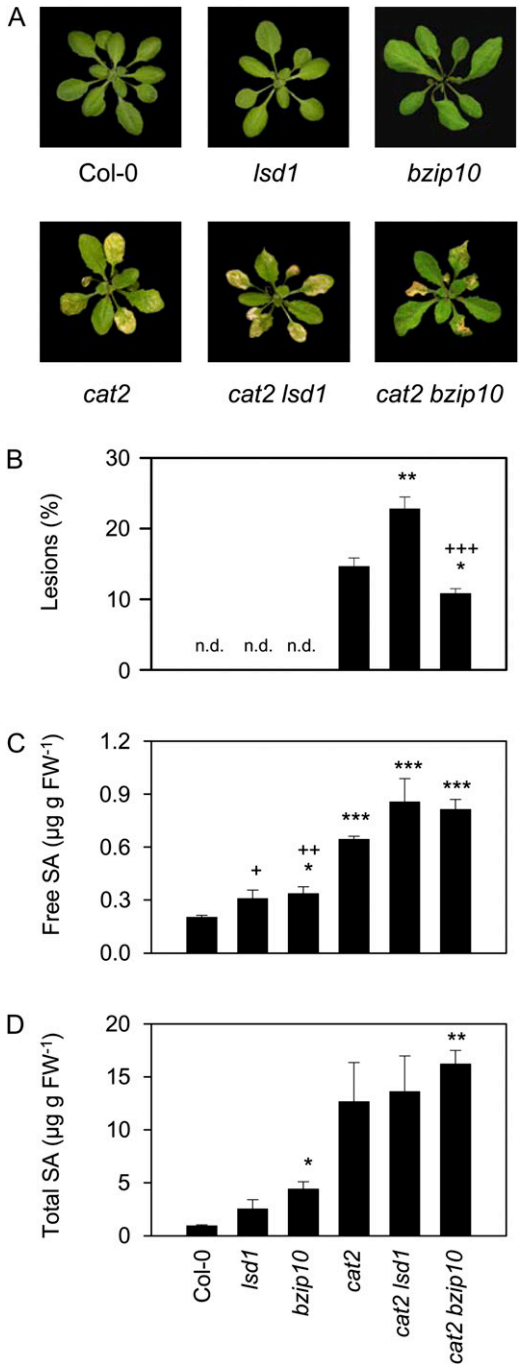

Figure 2. Phenotypes and SA contents of *cat2* crossed with *lsd1* and *bzip10* and grown in LD. A, Photographs of plants. B, Lesion extent in the different genotypes, quantified as percentage rosette leaf area. n.d., Not detected. C, Free SA contents in the different lines. D, Total SA (free + glucoside) contents in the different lines. Significant differences from Col-0 are indicated by * $P < 0.05$, ** $P < 0.01$, and *** $P < 0.001$, while significant differences of other genotypes from *cat2* are indicated by $^{+}$ $P < 0.05$, $^{++}$ $P < 0.01$, and $^{+++}$ $P < 0.001$. FW, Fresh weight. [See online article for color version of this figure.]

the detected compounds were affected by the *cat2* mutation; (2) that the effect of the *cat2* mutation was highly dependent on daylength; and (3) that the introduction of the *sid2* mutation into the *cat2* background greatly altered H_2O_2-dependent metabolite profiles in LD. Thus, similar to its effect on glutathione status (Fig. 3E), the *sid2* mutation reversed the LD-specific effects of H_2O_2 on metabolite profiles. This is illustrated by principal component analysis (Fig. 4B), which segregated *cat2* background samples (within the blue outer ellipse) from Col-0 and *sid2* samples. Strikingly, the analysis further subdivided *cat2* background samples into *cat2* grown in LD (black squares contained in the orange ellipse) from the other nine *cat2* and *cat2 sid2* samples (triangles and red squares grouped in the blue inner ellipse). Thus, metabolite profiling was able to clearly separate plants showing LD- and SA-dependent cell death from those undergoing oxidative stress without the formation of spreading lesions (Fig. 4B).

Further *t* tests were performed to identify (1) metabolites that were modulated by H_2O_2 independently of daylength and ICS1 function and (2) compounds whose abundance was influenced by H_2O_2 in a manner dependent on ICS1 and daylength (see "Materials and Methods"). The first group of metabolites, denoted "oxidative stress profile," corresponded to the effect of the *cat2* mutation in both conditions (SD and LD) and both genotypes (*cat2* and *cat2 sid2*); that is, it opposed all *cat2* and *cat2 sid2* extracts (sample group A) to all *sid2* and Col-0 extracts (sample group B), as shown in Supplemental Table S1. Metabolites that showed significant differences in this analysis can be functionally linked to the decreased growth phenotype. The second group, designated "defense/death profile," describes metabolites that distinguish *cat2* in LD (sample group A) from all other samples (sample group B), as shown in Supplemental Table S2, and is linked with the presence or absence of lesions. Only nine of 106 metabolites showed the oxidative stress profile, and of these, only one (Fru) was also included in the defense/death profile (Fig. 4C). Among the 50 metabolites that showed the defense/death profile but not the oxidative stress profile were SA (in agreement with the HPLC analysis; Fig. 1), azelaic acid, putrescine, and the aromatic amino acids Trp, Tyr, and Phe, as well as Lys. These metabolites specifically accumulated in *cat2* in LD (Fig. 4C).

Genetic Reversion of Pathogen Responses and Gene Expression Profiles in *cat2*

Consistent with its effect in preventing H_2O_2-triggered SA synthesis in *cat2* in LD, the *sid2* mutation abolished *PR1* induction (Fig. 5A). The lipid transfer protein AZI1 has recently been shown to prime the SA response (Jung et al., 2009). Consistent with this role and the accumulation pattern of azelaic acid (Fig. 4C), *AZI1* transcripts were induced in *cat2* in LD (Fig. 5B). However, in *cat2 sid2* plants, this induction was

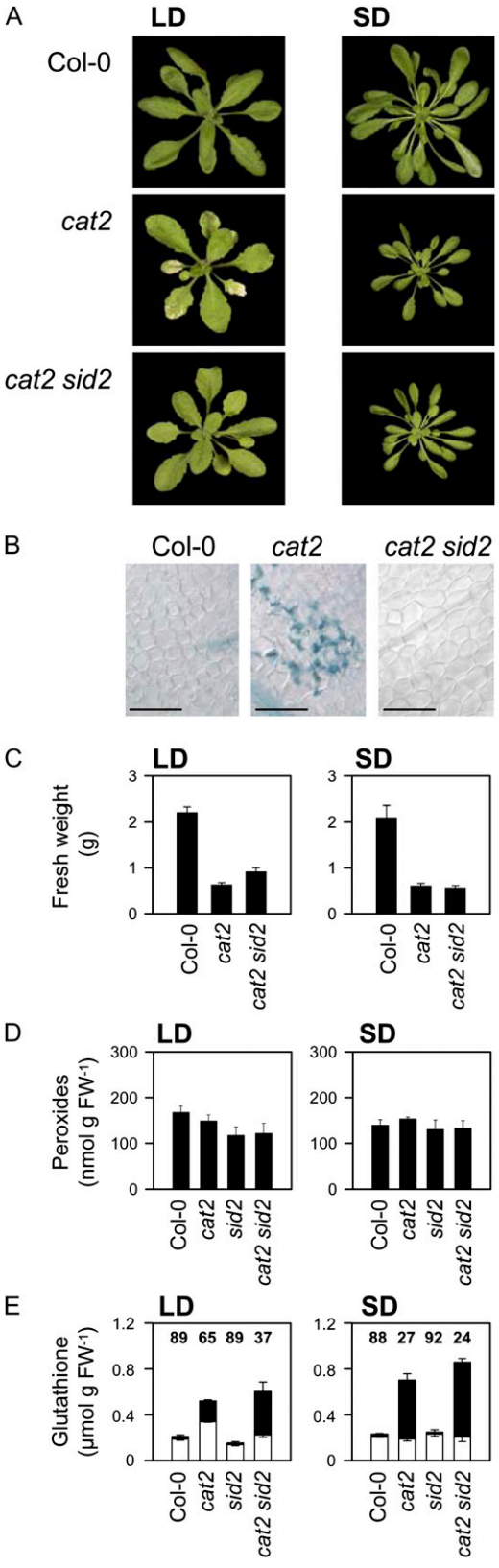

Figure 3. Reversion of LD-dependent lesions in *cat2* by crossing with the *sid2* mutant. A, Phenotypes of rosettes of plants after 25 d of growth in LD or 40 d of growth in SD. B, Trypan blue staining of *cat2* and *cat2 sid2* leaves grown in LD conditions. No staining was observed in any of the genotypes grown in SD. Bars = 200 μm. C, Rosette fresh weight (g) of Col-0, *cat2*, and *cat2 sid2* grown in LD or SD. Data represent means ± SE (n = 10–12). D, Extractable leaf peroxide contents in all four genotypes. E, Glutathione contents. White and black bars represent reduced and oxidized glutathione, respectively. Numbers indicate percentage of glutathione in the reduced form. For D and E, data are means ± SE of three independent extracts. FW, Fresh weight. [See online article for color version of this figure.]

abolished. A similar expression pattern was observed for two CYP450s involved in camalexin synthesis (Glawischnig, 2007; Nafisi et al., 2007) as well as for camalexin itself and both free and total scopoletin (Fig. 5, C–G). Thus, a wide range of pathogen responses induced by intracellular H_2O_2 was annulled by the *sid2* mutation. However, these ICS1-dependent responses in *cat2* were not associated with the induction of *ICS1* at the transcript level (Fig. 5H).

By cDNA-amplified fragment length polymorphism (AFLP) analysis, we extended the identification of transcripts involved in the daylength- and ICS1-dependent oxidative stress response. Using primer combinations that allow the amplification of stress- and defense-related sequences (Queval et al., 2007; Vuylsteke et al., 2007), the expression of approximately 2,000 transcripts was monitored in Col-0, *sid2*, *cat2*, and *cat2 sid2* grown in LD. Because the *sid2* mutation had little impact on the *cat2* phenotype or metabolite profiles in SD, we omitted this condition from the analysis. Significant differences in abundance were found for 534 fragments (ANOVA, $P < 0.05$), and clustering of these fragments revealed that while some genes were induced in *cat2* independently of *sid2*, the majority were influenced by the *sid2* mutation (Fig. 6A). For 58 fragments, sequence information was retrieved (Supplemental Table S3). The expression patterns of four representative transcripts were confirmed by quantitative (q)PCR analysis on samples obtained from a second independent experiment (Fig. 6B). While the H_2O_2 marker *GSTU24* (Vanderauwera et al., 2005) was induced similarly in *cat2* and *cat2 sid2*, other genes involved in antioxidative metabolism were exclusively induced by H_2O_2 when ICS1 was functional. These included a Met sulfoxide reductase (Fig. 6B) and a monodehydroascorbate reductase (Supplemental Table S3), suggesting that cell death in *cat2* is not caused by withdrawal of recognized antioxidative defenses.

Complementation of H_2O_2-Triggered Lesion Formation in Nonpermissive Conditions by SA

To test whether lesion formation in *cat2* could be restored in SD conditions, which are otherwise nonpermissive for cell death in *cat2*, SA complementation experiments were undertaken. First, we checked whether lesion formation could be restored in *cat2 sid2* in LD. Treatment with SA (at concentrations that did not affect Col-0) did not greatly affect the phenotype of *cat2* but induced lesion formation in *cat2 sid2*

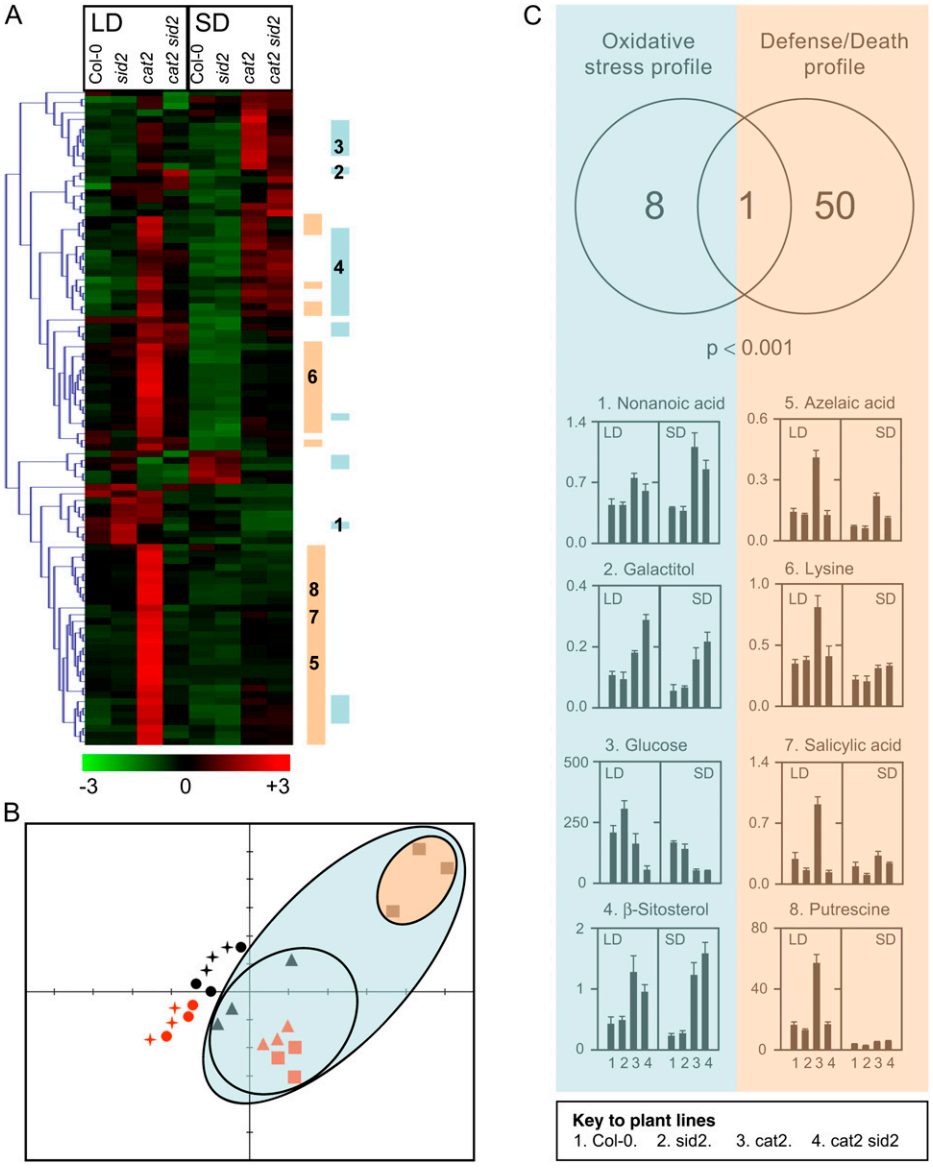

Figure 4. Metabolite profiling of Col-0, *sid2*, *cat2*, and *cat2 sid2* grown in LD and SD. A, Hierarchical clustering of significant differentially accumulated metabolites (ANOVA, $P < 0.05$) between different sample types (different genotypes in SD or LD, triplicate samples). Mean metabolite abundance for each sample type is shown by red (high abundance) or green (low abundance). Blue bars indicate metabolites that are strongly associated with oxidative stress (*t* test, $P < 0.001$ when comparing *cat2* and *cat2 sid2* [$n = 12$] with Col-0 and *sid2* [$n = 12$]). Orange bars indicate metabolites that are strongly associated with lesion formation (*t* test, $P < 0.001$ when comparing *cat2* in LD [$n = 3$] with all other samples [$n = 21$]). B, Principal component analysis of GC-MS profiles of all 24 extracts (triplicate biological repeats of Col-0 [circles], *sid2* [stars], *cat2* [squares], and *cat sid2* [triangles] grown in LD [black] or SD [red]). C, Summary and representative histograms that show an oxidative stress profile (associated with *cat2* and *cat2 sid2* genotypes independent of photoperiod) or a defense/death profile (associated with *cat2* only in LDs). Background color and numbers of metabolites shown in histograms correspond to the labeling in the heat map shown in A.

with a similar pattern to that observed in *cat2* (Supplemental Fig. S3). Addition of SA promoted a less perturbed glutathione pool that was both decreased and less oxidized than in the absence of SA (Supplemental Fig. S3).

Despite the absence of cell death in *cat2* in SD even at elevated irradiance (Queval et al., 2007), SA treatment of *cat2* in SD under moderate irradiance induced lesion formation (Fig. 7A). This effect was not linked to greater glutathione oxidation (Fig. 7B). Another cellular redox buffer, ascorbate, was not affected by SA treatment (Fig. 7C).

Next, we analyzed whether SA treatment of *cat2* in SD restored the LD-dependent accumulation of camalexin and scopoletin. Whereas no significant accumulation of either compound was observed in SD in any of the water-treated plants, SA treatment induced both forms of scopoletin in both Col-0 and *cat2*, although the effect was stronger in the latter (Fig. 7D). The SA-induced increase in scopoletin was about 10-fold in Col-0 but about 30-fold in *cat2*. In contrast to scopoletin accumulation, which could be induced by SA treatment of all three genotypes, exogenous SA only induced camalexin production in *cat2* and *cat2 sid2* (Fig. 7D).

To investigate whether daylength-dependent activation of defense responses by photorespiratory H_2O_2 was reversible, plants were first grown in LD to initiate the accumulation of SA, associated defense compounds, and lesion formation. When lesions were clearly visible, plants were transferred to SD conditions. Transfer to SD arrested cell death and decreased free and total forms of SA and scopoletin (Fig. 8). Camalexin contents in *cat2* also decreased after transfer from LD to SD, and this effect was correlated with the decrease in free SA (Fig. 8). One week after transfer

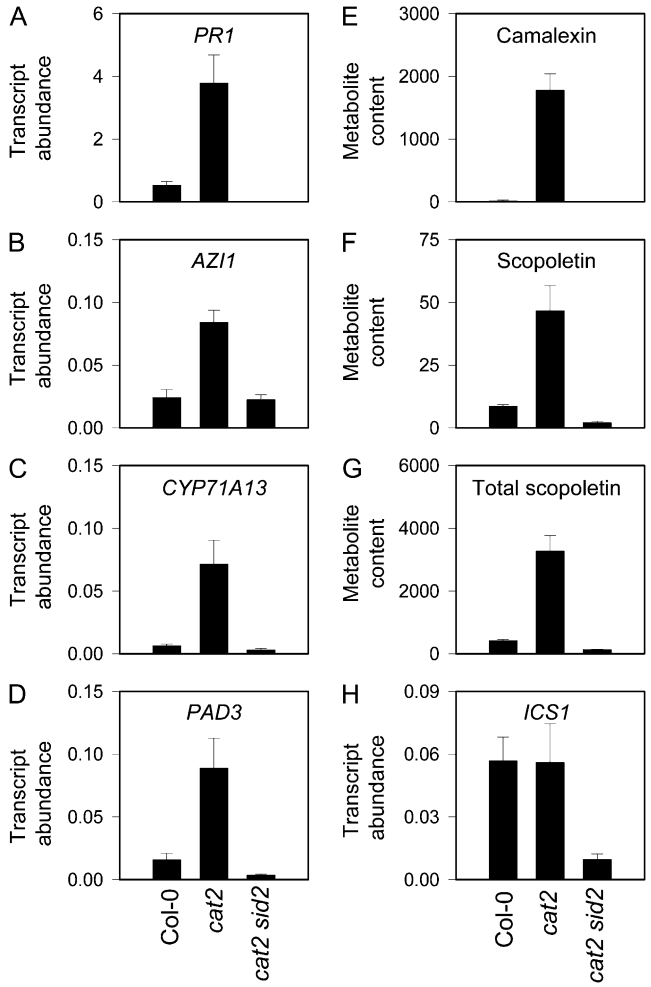

Figure 5. Suppression of defense responses in *cat2* by the *sid2* mutation. A to D and H, Transcript abundance of defense-related marker genes, measured by qPCR and expressed relative to *ACTIN2* abundance. E to G, Metabolite contents in ng g^{-1} fresh weight. Data are means ± SE of three independent extracts. A, *PR1* (At2g14610). B, *AZI1* (At4g12470). C, *CYP71A13* (At2g30770). D, *PAD3* (At3g26830). E, Camalexin. F, Scopoletin. G, Total scopoletin. H, *ICS1* (At1g74710).

to SD, defense-related metabolites had returned almost to Col-0 values (Fig. 8); that is, to values that are observed in *cat2* grown in SD from germination (Fig. 1).

Daylength Dependence of Resistance to Virulent Bacteria in *cat2*

The above observations show that the *cat2* mutation activates pathogen responses that are often induced following an incompatible interaction and that confer basal resistance to subsequent biotic challenge. Thus, the responses of Col-0 and *cat2* to a virulent strain of *Pseudomonas syringae* were tested in SD and LD conditions. No difference between the genotypes was apparent in SD (Fig. 9A, left), while in LD conditions, which are permissive for induction of SA, *PR1*, and phytoalexin (Fig. 1), *cat2* showed greater resistance than Col-0 (Fig. 9A, right).

We analyzed whether exogenous SA induces resistance in *cat2* in SD and in *cat2 sid2*. Whereas SA treatment enhanced resistance in both *cat2* and *cat2 sid2* in SD (Fig. 9B, left), it did not significantly further affect resistance in *cat2* in LD (Fig. 9B, right). SA treatment of *cat2 sid2* in LD restored resistance to the level observed in *cat2* in this condition (Fig. 9B, right).

DISCUSSION

Catalase-deficient plants have been used as a model to identify how plants respond to H_2O_2. These studies have shown that catalase deficiency in tobacco and Arabidopsis mimics many of the effects of environmental stresses on gene expression and on redox homeostasis (Willekens et al., 1997; Chamnongpol et al., 1998; Mittler et al., 1999; Vandenabeele et al., 2004; Vanderauwera et al., 2005; Queval et al., 2007). While many mutants that show spontaneous lesion formation have been described (Dietrich et al., 1994; Lorrain et al., 2003; Brodersen et al., 2005; Meng et al., 2009), questions remain concerning the relationship of the affected genes to changes in ROS availability, which are known to be important in the responses of plants to stress. Unlike many lesion-mimic mutants, increased H_2O_2 availability is unambiguously the initiating signal of responses in catalase-deficient plants. Studies of catalase-deficient plants, therefore, allow the specific influence of oxidative stress signaling pathways to be investigated.

Lesions Driven by Intracellular H_2O_2 Require SA Synthesis through the Isochorismate Pathway

SA is implicated in defense responses, including cell death (Vlot et al., 2009). In some lesion-mimic mutants, a link with SA has been demonstrated, although in several cases the role of SA itself is less clear (Hunt et al., 1997; Lorrain et al., 2003; Brodersen et al., 2005; Meng et al., 2009). Previous studies showed that SA accumulates in catalase-deficient tobacco (Takahashi et al., 1997; Chamnongpol et al., 1998). Using *nahG* lines, it was concluded that SA accumulation is required for *PR1* induction but not for lesion formation (Takahashi et al., 1997). This result suggested that cell death in catalase-deficient plants may be an inevitable consequence of excess cellular oxidation. If so, this would be consistent with the widespread notion that ROS cause tissue injury through chemically inevitable oxidative damage. Nevertheless, subsequent work in catalase-deficient tobacco provided evidence that death occurs through an active process (Dat et al., 2003). In this study, we sought to examine (1) whether H_2O_2-induced SA accumulation could be prevented and (2) whether this would affect H_2O_2-triggered cell death in Arabidopsis.

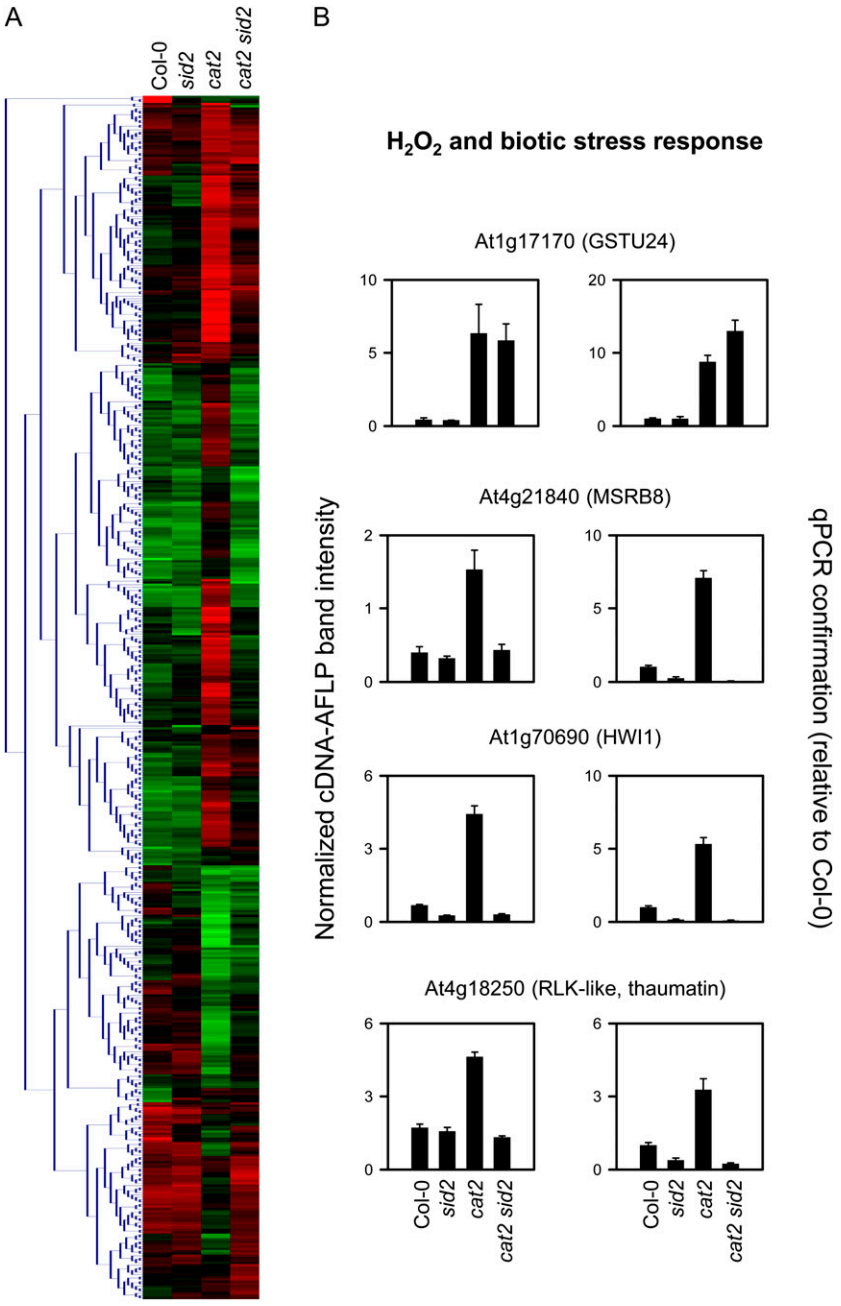

Figure 6. Transcript profiling of *cat2* and *cat2 sid2* plants. A, Hierarchical clustering of statistically different fragments identified by cDNA-AFLP analysis of Col-0, *sid2*, *cat2*, and *cat2 sid2* in LD conditions. B, Histograms show absolute expression levels of selected differentially expressed sequenced fragments (left) and qPCR confirmation of responses in an independent experiment (right).

Previous studies in tobacco did not identify the source of SA that accumulates when catalase is deficient. Use of *nahG* to diminish SA accumulation makes chemical complementation studies difficult (Lawton et al., 1995) and can also produce potentially interfering metabolites (Van Wees and Glazebrook, 2003). For these reasons, we decided to prevent SA accumulation by blocking SA synthesis in *cat2*. SA can be synthesized in Arabidopsis through pathways involving Phe ammonia lyase or ICS. Since the isochorismate pathway has been shown to be an essential source of SA during pathogen interactions (Wildermuth et al., 2001), we used the *sid2-1* line, which is defective in ICS1 activity (Nawrath and Métraux, 1999). This approach revealed that lesions triggered by intracellular H_2O_2-induced stress can be genetically reverted and therefore are not driven by widespread unspecific oxidation reactions. This is evidenced by comparison of the intracellular redox state in *cat2* and *cat2 sid2*. Intracellular thiol-disulfide status was more perturbed in the absence of ICS1-dependent SA accumulation and became less perturbed when SA was supplied exogenously. These observations suggest that SA does not couple intracellular H_2O_2 to lesions through enhanced, generalized, intracellular oxidation. Therefore, they argue against a simple oxidative stress model in which H_2O_2 activates SA synthesis, which then acts by aggravating oxidative stress.

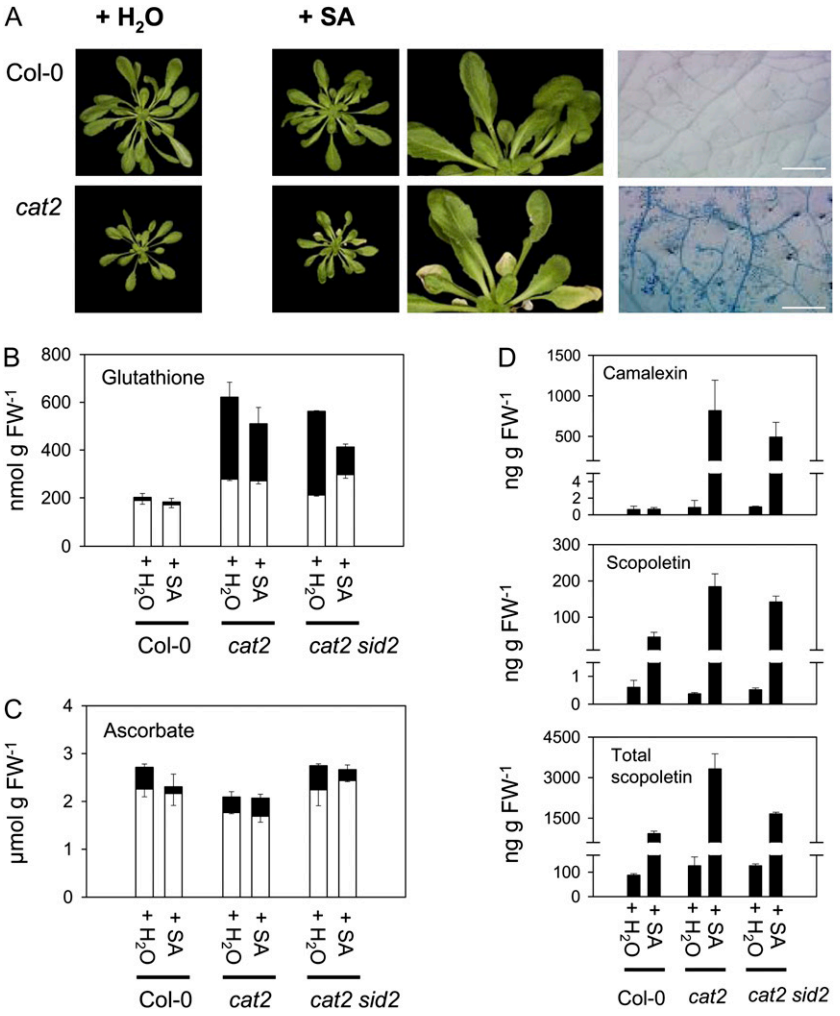

Figure 7. Complementation with exogenous SA induces cell death and defense compounds in *cat2* in SD. A, Phenotype of Col-0 and *cat2* plants grown in SD and sprayed with 1 mM SA or with water. Exogenous SA had no effect on *sid2* or Col-0. Bars = 1 mm. B, Leaf glutathione. White bars show reduced glutathione; black bars show oxidized glutathione. C, Leaf ascorbate. White bars show ascorbate; black bars show dehydroascorbate. D, Camalexin and free and total scopoletin contents. For B to D, data are means ± SE of three independent leaf extracts taken from different plants. FW, Fresh weight. [See online article for color version of this figure.]

As well as SA, the only other clearly identified metabolite synthesized from isochorismate in Arabidopsis is the PSI electron acceptor, phylloquinone. While ICS1 is the major source of SA, there is partial redundancy with ICS2 in phylloquinone production (Garcion et al., 2008). Decreased phylloquinone synthesis in *sid2* is unlikely to explain our observations. First, no differences in growth rates were observed between Col-0 and *sid2* in standard conditions (SD and LD in air). Second, growth rates were similar in all lines at high CO_2, a condition in which the *cat2* mutation is silent. Third, and most crucially, lesion formation was restored in *cat2 sid2* in LD and induced in *cat2* in SD by complementation with SA.

Peroxisomal H_2O_2 Induces Biotic Defense Response Markers in *cat2* Specifically in LD

Our data show that pathogen responses triggered by intracellular oxidative stress are influenced by growth daylength (Fig. 10). Studies on the *lsd1* mutant have reported daylength dependence of lesion formation (Dietrich et al., 1994), and cell death in *cat2* is also mediated partly through the *LSD1-bZIP10* pathway. This suggests that LD-dependent lesions in *cat2* occur through a programmed cell death process similar to the hypersensitive response that occurs during incompatible plant-pathogen interactions.

A key question is whether the daylength dependence of responses in *cat2* reflects the intensity of oxidative stress or additional signals that modulate the response to this stress. Our analysis of intracellular redox markers provides little evidence for enhanced oxidative perturbation in *cat2* in LD compared with *cat2* in SD or *cat2 sid2* in LD. Thus, leaf cells can cope with marked perturbation of intracellular redox state without undergoing cell death. Strikingly, LD-dependent defense responses were down-regulated within days of transferring *cat2* to SD conditions (Fig. 8), indicating that these effects are mediated through reversible signaling pathways rather than simply requiring a threshold stress intensity for initiation. One possibility is that the plant is able to sense the duration of H_2O_2 exposure (rather than the degree of stress at any given time). While this remains an intriguing possibility, our previous analyses suggest that the

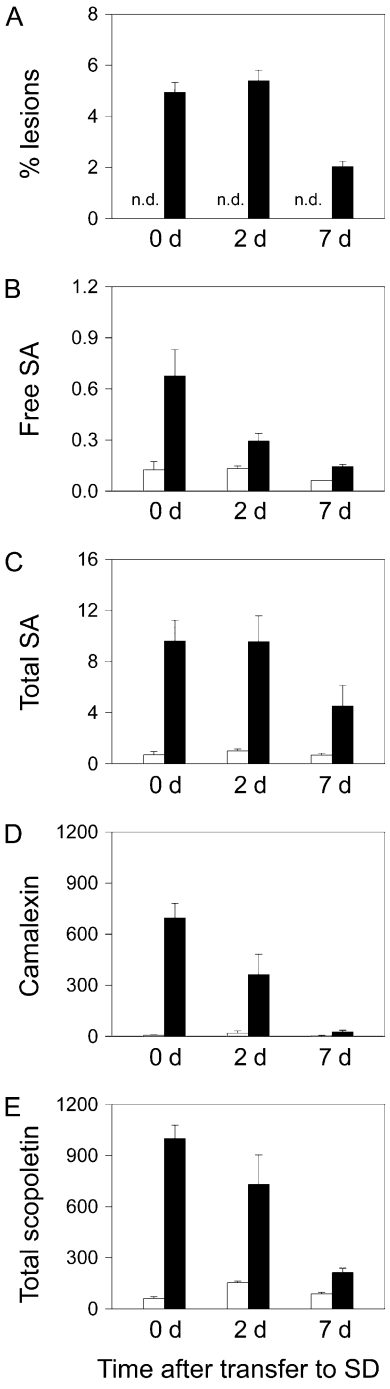

Figure 8. Reversibility of LD-dependent defense responses in *cat2* by transfer to SD. Col-0 (white bars) and *cat2* (black bars) were grown in LD until lesion formation was visible in *cat2* (21 d after germination). Plants were then transferred to SD, and lesions and defense compounds were monitored after 2 and 7 d. A, Lesion quantification, expressed as percentage of rosette area. n.d., Not detected. B, Free SA (μg g^{-1} fresh weight). C, Total SA (μg g^{-1} fresh weight). D, Camalexin (ng g^{-1} fresh weight). E, Total scopoletin (ng g^{-1} fresh weight). Data are means ± SE of three independent leaf extracts taken from different plants.

conditionality of lesion formation in *cat2* is partly linked to daylength perception independent of the duration of exposure to H_2O_2 (Queval et al., 2007). Consistent with this explanation, it has recently been reported that longer daylengths increase leaf injury induced by equal-time ozone exposures (Vollsnes et al., 2009). Because there is evidence for overlap between SA, pathogen responses, and the regulation of flowering (Martínez et al., 2004), the requirement for LD-dependent SA accumulation in *cat2* may reflect the coordination of H_2O_2-triggered lesions with the flowering program. Some aspects of pathogen responses interact with or are influenced by the phytochrome pathway (Genoud et al., 2002; Griebel and Zeier, 2008), while cryptochrome has been implicated in singlet oxygen-mediated effects (Danon et al., 2006). Thus, the daylength dependence of responses in *cat2* (Fig. 10) could reflect an influence of photoreceptor pathways, perception of the duration of increased H_2O_2 availability, or both factors operating in concert.

Although *ICS1* transcripts are induced during pathogen challenge (Wildermuth et al., 2001), no such induction was associated with *ICS1*-dependent pathogen responses in *cat2* (Fig. 5). It is possible that *ICS1* transcript induction is a transient phenomenon that was not detected in our study. An alternative possibility is that the regulation of the chloroplastic isochorismate pathway is redox dependent at the posttranscriptional

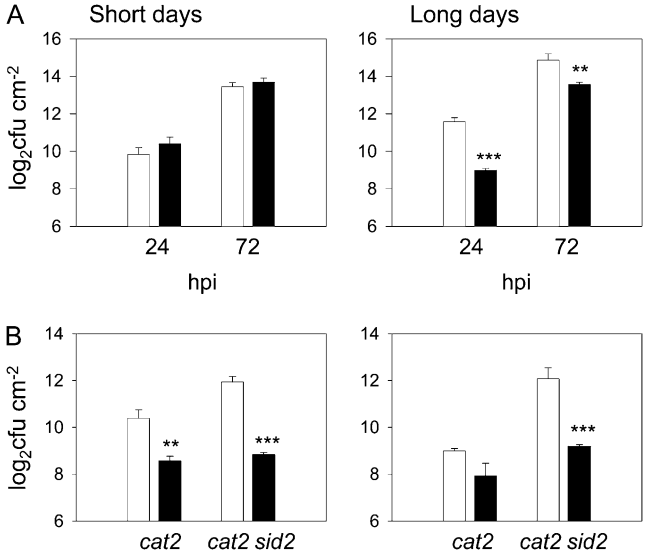

Figure 9. Effect of the *cat2* mutation on Arabidopsis resistance to virulent bacteria in SD and LD conditions. A, Growth of *P. syringae* pv *tomato* DC3000 in leaves of Col-0 (white bars) and *cat2* (black bars) growing in SD or LD. Significant *cat2*/Col-0 differences are indicated by asterisks: ** $P < 0.01$, *** $P < 0.001$. cfu, Colony-forming units; hpi, hours post inoculation. B, Bacterial growth in *cat2* and *cat2 sid2* supplemented with exogenous SA. Plants grown in SD (left) or LD (right) were sprayed or not with 1 mM SA on 2 successive days preceding inoculation. White bars show untreated; black bars show SA treated. Significant differences between SA-treated and untreated are indicated by asterisks: ** $P < 0.01$, *** $P < 0.001$.

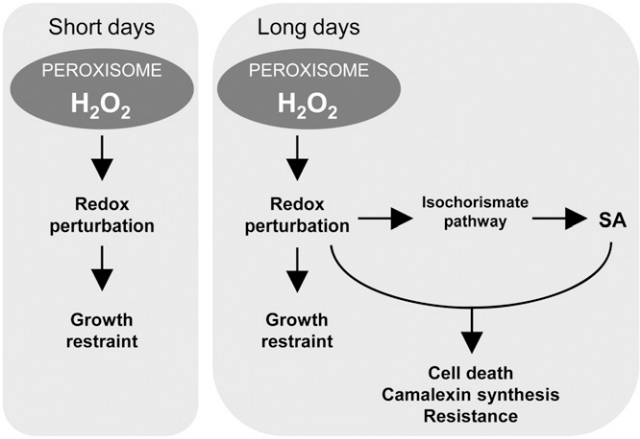

Figure 10. Scheme showing the role of daylength and SA in the control of responses driven by peroxisomal H_2O_2. Independent of the daylength, intracellular oxidative stress restrains growth. In LD conditions, activation of the isochorismate pathway allows peroxisome-sourced oxidative stress and SA to function together to induce cell death and other pathogen responses.

level, a phenomenon that has been described for the cytosolic protein NPR1 (Tada et al., 2008).

Differential Control of Defense Metabolites by H_2O_2 and SA: Camalexin Accumulation Requires Both Signals

The daylength conditionality of phenotypic responses to H_2O_2 in *cat2*, and their dependence on SA, enabled us to analyze the interaction between these two compounds in influencing metabolite contents. Metabolites that were affected by H_2O_2 independently of SA (oxidative stress profile) included Glc, Fru, myoinositol, and galactinol, all of which were decreased in *cat2* (Fig. 4; Supplemental Table S1). The last two of these metabolites are involved in the raffinose synthesis pathway, which may play an antioxidative role (Nishizawa et al., 2008).

A large group of compounds detected by GC-MS showed a "defense/death" profile; that is, they were only affected by H_2O_2 in an LD- and SA-dependent manner. Among these was azelaic acid. This compound was recently shown to prime plant defense, notably promoting the induction of *AZI1* transcripts and SA accumulation (Jung et al., 2009). Thus, intracellular H_2O_2 is able to drive production of this compound and *AZI1* up-regulation, but these effects require SA accumulation through ICS1, suggesting two-way cross talk between SA and azelaic acid. Several compounds showing a similar profile were amino acids. This may to some extent reflect SA-induced protein turnover. However, amino acids synthesized by the shikimate pathway, as well as shikimic acid itself, were among these compounds. Phe is the precursor for the pathogen-induced coumarin scopoletin (Chong et al., 2002), while Trp is the precursor for camalexin (Glawischnig, 2007). The precise roles of H_2O_2 and SA in regulating the accumulation of these two secondary metabolites are unclear. Our analysis suggests that scopoletin accumulation is largely under SA control but is reinforced by H_2O_2 (Fig. 7).

Camalexin accumulation has previously been reported to require other signals as well as SA (Zhao and Last, 1996; Zhou et al., 1998; Thomma et al., 1999). However, another view is that accumulation of this compound simply requires ROS production (Kliebenstein, 2004; Glawischnig, 2007). Because the *cat2* mutation enables H_2O_2 and SA synthesis to be conditionally and genetically separated, we have been able to show that significant camalexin accumulation requires the simultaneous presence of both signals (Fig. 7). This requirement likely explains the failure of oxidative stress to induce camalexin in *cat2* in SD (insufficient SA) as well as previous studies in which SA treatment alone is not sufficient (absence of an H_2O_2 signal). The absolute requirement of both signals for camalexin accumulation is further evidence against the notion that SA functions through a simple aggravation of oxidative stress, a conclusion supported by the fact that exogenous SA did not increase oxidation of either ascorbate or glutathione in any of the genotypes tested (Fig. 7).

A Role for Photorespiratory H_2O_2 in Pathogen Responses in Wild-Type Plants?

This study identifies *cat2* as a constitutive defense mutant in LD that is a model line in which to delineate the specific function of H_2O_2 from other processes during biotic interactions. The generalized production of H_2O_2 in leaf cells in *cat2* enables defense responses to be studied without the spatial constraints associated with the more localized processes that occur during infection. Plant-pathogen interactions are known to be influenced by light (Bechtold et al., 2005; Torres et al., 2006), and this could at least partly reflect the light dependence of ROS production. The primary focus on the origin of H_2O_2 during pathogen interactions has been on the plasmalemma/apoplast, with most attention paid to NADPH oxidases. However, plant cells can produce ROS through numerous other intracellular and extracellular sources. Peroxisomes are important in the production of signal molecules, including ROS (del Río et al., 2006; Nyathi and Baker, 2006). Particularly in the leaves of C_3 plants, these organelles can be a rich source of H_2O_2 through the photorespiratory glycolate oxidase reaction (Noctor et al., 2002). A role for peroxisomal H_2O_2 in pathogen responses is consistent with studies of mutants for Ser:glyoxylate aminotransferase (Taler et al., 2004), an enzyme immediately downstream of glycolate oxidase in the photorespiratory pathway, as well as effects of photorespiratory conditions on the phenotypes of the *lsd1* mutant (Mateo et al., 2004). Given the high catalase activities of wild-type plants, it is likely that this enzyme must be down-regulated to allow H_2O_2 produced in leaf peroxisomes to contribute to signaling

during a biotic challenge (Foyer et al., 2009). Several mechanisms by which this could occur have been described. Transcripts for tobacco *CAT1* (equivalent to Arabidopsis *CAT2*) were strongly down-regulated during infection (Dorey et al., 1998). Furthermore, stress conditions cause down-regulation of catalase through slowed protein resynthesis (Volk and Feierabend, 1989), and SA itself has been described as a catalase inhibitor (Vlot et al., 2009). Other catalase inhibitors may play roles during certain plant-pathogen interactions (Beffagna and Lutzu, 2007), while selective degradation of peroxisomal catalase was reported to be the major mechanism allowing ROS accumulation to trigger autophagic programmed cell death in a mouse cell line (Yu et al., 2006). Therefore, these elements suggest that our observations in *cat2* are relevant to processes occurring in wild-type plants undergoing ROS-triggered cell death.

MATERIALS AND METHODS

Plant Material

T-DNA and other mutant lines of Arabidopsis (*Arabidopsis thaliana*) were all in the Col-0 background. The *cat2* line was *cat2-2* (Queval et al., 2007), now renamed *cat2-1* (Queval et al., 2009). The *LSD1* mutant (*lsd1-2*) was a kind gift from Miguel Torres and Jeff Dangl (University of North Carolina). A *bzip10* insertion mutant (SALK_014867; Kaminaka et al., 2006) was obtained from public seed banks. Homozygotes were identified using sequence information obtained from the SIGnAL Web site at http://signal.salk.edu, and seeds were obtained from the Nottingham Arabidopsis Stock Centre (http://nasc.nott.ac.uk).

Identification of Homozygous Double Mutants

Homozygotes for *lsd1*, *bzip10*, and *sid2* were crossed with *cat2*. After verification of double heterozygotes in the F1 generation, double homozygotes were identified in plants grown from F2 seeds. Leaf DNA was amplified by PCR (30 s at 94°C, 30 s at 60°C, 1 min at 72°C, 30 cycles) using primers specific for left T-DNA borders and the *CAT2*, *LSD1*, and *bZIP10* genes (Supplemental Table S4). Zygosity was analyzed by PCR amplification of leaf DNA as shown in Supplemental Figure S1 for *cat2*. Zygosity of the *sid2* mutation was established using restriction length polymorphism (Supplemental Fig. S1). All further analyses were performed on plants grown from double homozygote F3 seeds.

Plant Growth and Sampling

Plants were grown in a controlled-environment growth room either at a day/night regime of 8 h/16 h (SD) or 16 h/8 h (LD), an irradiance of 200 μmol quanta m^{-2} s^{-1} at leaf level, 20°C day/18°C night, 65% humidity, CO_2 at 400 μL L^{-1}, and given nutrient solution twice per week. Where indicated, CO_2 was enriched to 3,000 μL L^{-1} ("high CO_2"). Plants were analyzed and sampled at the age of 21 to 24 d (LD) and 42 d (SD). For SA complementation experiments, rosettes were sprayed with 1 mM SA every 2 d for 8 d in LD and 14 d in SD. Samples from at least three different plants were taken in the middle of the photoperiod, rapidly frozen in liquid nitrogen, and stored at −80°C until analysis. Unless otherwise stated, data are means ± SE of three to four independent samples from different plants, and significant differences are expressed using Student's *t* test at $P < 0.05$, $P < 0.01$, and $P < 0.001$. All experiments were repeated at least twice with similar results.

Lesion Detection and Pathogen Tests

Dead cells were stained in detached rosette leaves as described (Queval et al., 2007) using a method modified from Wäspi et al. (2001). Percentage lesion areas were quantified using IQmaterials software. For resistance tests, the virulent *Pseudomonas syringae* pv *tomato* strain DC3000 was used in a medium titer of 5×10^5 colony-forming units mL^{-1}. Whole leaves of 3- and 5-week-old plants grown in SD or LD were infiltrated using a 1-mL syringe without a needle in the middle of the photoperiod, and leaf discs were taken for analysis at the same time point on subsequent days. For SA complementation experiments, plants were sprayed with 1 mM SA solution on 2 successive days preceding inoculation. Leaf discs (0.5 cm^2 each) were harvested from inoculated leaves. For each time point, four samples were made by pooling two leaf discs from different plants. Bacterial growth was assessed by homogenizing leaf discs in 400 μL of water, plating appropriate dilutions on solid King B medium containing rifampicin and kanamycin, and quantifying colony numbers after 3 d.

qPCR Analysis

To quantify pathogen defense-related transcripts (Fig. 5), RNA was extracted using the NucleoSpin RNA Plant Kit (Macherey-Nagel) and reverse transcribed with the SuperScript III First-Strand Synthesis System (Invitrogen). qPCR was performed according to Queval et al. (2007). Primer sequences are listed in Supplemental Table S4.

cDNA-AFLP Analysis

cDNA-AFLP analysis was performed on plants grown in a 16-h photoperiod. For each genotype, duplicate samples were analyzed, each consisting of pooled material from at least three different plants. Templates for cDNA-AFLP were prepared, amplified, and quantified as described by Queval et al. (2007). Next, a coefficient of variation (CV) was calculated by dividing the SD across all samples by the mean for each band. Bands showing the lowest CV values across all samples were considered as constitutive genes and were used to normalize bands showing higher CV values. To identify fragments showing significant intergenotype variation, one-way ANOVA was used at $P < 0.05$. Significant fragments were centered by division of the mean value for each sample type by the mean value of all samples and reduced by division with the SD across all samples, and hierarchical clustering was performed. In total, bands of 58 significantly differentially expressed fragments were excised from the gels and reamplified by PCR with the respective selective cDNA-AFLP primers. PCR fragments were directly sequenced. Expression characteristics of four genes were validated on three independent replicates of a biological repeat experiment using qPCR analysis as described in Supplemental Table S4.

Metabolite Measurements

Peroxides were measured by luminol luminescence according to Queval et al. (2008). Tissue samples of 50 mg fresh weight were ground to a fine powder in liquid nitrogen and then extracted into 1 mL of 0.2 N HCl. The homogenate was centrifuged for 10 min at 10,000*g*. The extract was neutralized to pH 5.6 with 0.2 M NaOH. To avoid interference from ascorbate, an aliquot (50 μL) was treated with ascorbate oxidase, and the treated aliquot was added to 0.5 mL of 0.2 M NH_3, pH 9.5, and 0.05 μL of 0.5 mM luminol (prepared in 0.2 M NH_3, pH 9.5), vortexed rapidly, and injected into a luminometer. The reaction was started by adding 100 μL of 0.5 mM $K_3Fe(CN)_6$ (in NH_3), and luminol chemiluminescence was monitored for 2 s. To check the linearity of this assay, a standard curve of H_2O_2 was done for each experiment, and assay standards and extracts were assayed in triplicate. Oxidized and reduced forms of glutathione and ascorbate were measured as described by Queval and Noctor (2007). Camalexin and free and total forms of SA and scopoletin were measured according to Langlois-Meurinne et al. (2005). Nontargeted metabolite profiling was performed on triplicate biological repeats as in Noctor et al. (2007), except that a mix of alkanes was included during derivatization to aid metabolite identification. Compounds identified by retention index were confirmed by reference to mass spectra libraries. Peak area was quantified based on specific fragments and was corrected on the basis of an internal standard (ribitol) and sample fresh weight. Normalized peak areas were subject to ANOVA ($P < 0.05$) to identify significantly different metabolites. To display metabolites that were significant at $P < 0.05$ (Fig. 4A), centered-reduced values were generated as detailed in Supplemental Tables S1 and S2. To identify the two profiles shown in Figure 4C, all 12 *cat2* samples (*cat2* SD, LD, *cat2 sid2* SD, LD) were subjected to *t* test at $P < 0.001$ against the

12 Col-0 and *sid2* samples to give oxidative stress profiles (Supplemental Table S1). The defense/death profile was obtained by *t* test ($P < 0.001$) of three *cat2* LD samples against the remaining 21 samples (Supplemental Table S2). False positive discovery was checked by testing groups of samples chosen at random (3×12 versus 3×12 or 3×3 versus 3×21) at $P < 0.001$. Of 106 metabolites tested, none was found to be significantly different in any of these control tests.

Supplemental Data

The following materials are available in the online version of this article.

Supplemental Figure S1. Genotyping and detection of *cat2* and *sid2* mutations.

Supplemental Figure S2. Phenotypes of Col-0, *sid2*, *cat2*, and *cat2 sid2* grown at high CO_2.

Supplemental Figure S3. Rescue of lesion formation in *cat2 sid2* in LD by complementation with exogenous SA.

Supplemental Table S1. List of metabolites that show an oxidative stress profile.

Supplemental Table S2. List of metabolites that show a defense/death profile.

Supplemental Table S3. Identified genes that show a significant inter-genotype difference in Col-0, *cat2*, *sid2*, and *cat2 sid2* in LD.

Supplemental Table S4. DNA primers used in this study.

ACKNOWLEDGMENTS

We thank the Salk Institute Genomic Analysis Laboratory for providing the sequence-indexed Arabidopsis T-DNA insertion mutants, the Nottingham Arabidopsis Stock Centre for supply of seed stocks, and Caroline Mauve for advice on GC-MS analysis.

Received January 29, 2010; accepted June 11, 2010; published June 11, 2010.

LITERATURE CITED

Bechtold U, Karpinski S, Mullineaux PM (2005) The influence of the light environment and photosynthesis on oxidative signalling responses in plant-biotrophic pathogen interactions. Plant Cell Environ **28:** 1046–1055

Beffagna N, Lutzu I (2007) Inhibition of catalase activity is an early response of *Arabidopsis thaliana* cultured cells to the phytotoxin fusicoccin. J Exp Bot **58:** 4183–4194

Bindschedler LV, Dewdney J, Blee KA, Stone JM, Asai T, Plotnikov J, Denoux C, Hayes T, Gerrish C, Davies DR, et al (2006) Peroxidase-dependent apoplastic oxidative burst in Arabidopsis required for pathogen resistance. Plant J **47:** 851–863

Brodersen P, Malinovsky FG, Hématy K, Newman MA, Mundy J (2005) The role of salicylic acid in the induction of cell death in Arabidopsis *acd11*. Plant Physiol **138:** 1037–1045

Chamnongpol S, Willekens H, Moeder W, Langebartels C, Sandermann H Jr, Van Montagu M, Inzé D, Van Camp W (1998) Defense activation and enhanced pathogen tolerance induced by H_2O_2 in transgenic plants. Proc Natl Acad Sci USA **95:** 5818–5823

Chong J, Baltz R, Schmitt C, Beffa R, Fritig B, Saindrenan P (2002) Downregulation of a pathogen-responsive tobacco UDP-Glc:phenylpropanoid glucosyltransferase reduces scopoletin glucoside accumulation, enhances oxidative stress, and weakens virus resistance. Plant Cell **14:** 1093–1107

Danon A, Sánchez Coll N, Apel K (2006) Cryptochrome-1-dependent execution of programmed cell death induced by singlet oxygen in *Arabidopsis thaliana*. Proc Natl Acad Sci USA **103:** 17036–17041

Dat JF, Pellinen R, Beeckman T, Van De Cotte B, Langebartels C, Kangasjärvi J, Inzé D, Van Breusegem F (2003) Changes in hydrogen peroxide homeostasis trigger an active cell death process in tobacco. Plant J **33:** 621–632

del Río LA, Sandalio LM, Corpas FJ, Palma JM, Barroso JB (2006) Reactive oxygen species and reactive nitrogen species in peroxisomes: production, scavenging, and role in cell signaling. Plant Physiol **141:** 330–335

Dietrich RA, Delaney TP, Uknes SJ, Ward ER, Ryals JA, Dangl JL (1994) Arabidopsis mutants simulating disease resistance response. Cell **77:** 565–577

Dorey S, Baillieul F, Saindrenan P, Fritig B, Kauffman S (1998) Tobacco class I and II catalases are differentially expressed during elicitor-induced hypersensitive cell death and localized acquired resistance. Mol Plant Microbe Interact **11:** 1102–1109

Foyer CH, Bloom AJ, Queval G, Noctor G (2009) Photorespiratory metabolism: genes, mutants, energetics, and redox signaling. Annu Rev Plant Biol **60:** 455–484

Foyer CH, Noctor G (2003) Redox sensing and signalling associated with reactive oxygen in chloroplasts, peroxisomes and mitochondria. Physiol Plant **119:** 355–364

Gapper C, Dolan L (2006) Control of plant development by reactive oxygen species. Plant Physiol **141:** 341–345

Garcion C, Lohmann A, Lamodière E, Catinot J, Buchala A, Doermann P, Métraux JP (2008) Characterization and biological function of the *ISOCHORISMATE SYNTHASE2* gene of Arabidopsis. Plant Physiol **147:** 1279–1287

Genoud T, Buchala AJ, Chua NH, Métraux JP (2002) Phytochrome signalling modulates the SA-perceptive pathway in *Arabidopsis*. Plant J **31:** 87–95

Glawischnig E (2007) Camalexin. Phytochemistry **68:** 401–406

Griebel T, Zeier J (2008) Light regulation and daytime dependency of inducible plant defenses in Arabidopsis: phytochrome signaling controls systemic acquired resistance rather than local defense. Plant Physiol **147:** 790–801

Hunt MD, Delaney TP, Dietrich RA, Weymann KB, Dangl JL, Ryals JA (1997) Salicylate-independent lesion formation in Arabidopsis *lsd* mutants. Mol Plant Microbe Interact **10:** 531–536

Jung HW, Tschaplinski TJ, Wang L, Glazebrook J, Greenberg JT (2009) Priming in systemic plant immunity. Science **324:** 89–91

Kaminaka H, Näke C, Epple E, Dittgen J, Schütze K, Chaban C, Holt BF III, Merkle T, Schäfer E, Harter K, et al (2006) bZIP10-LSD1 antagonism modulates basal defense and cell death in *Arabidopsis* following infection. EMBO J **25:** 4400–4411

Kliebenstein DJ (2004) Secondary metabolites and plant/environment interactions: a view through *Arabidopsis thaliana* tinged glasses. Plant Cell Environ **27:** 675–684

Lamb C, Dixon RA (1997) The oxidative burst in plant disease resistance. Annu Rev Plant Physiol Plant Mol Biol **48:** 251–275

Langlois-Meurinne M, Gachon CMM, Saindrenan P (2005) Pathogen-responsive expression of glycosyltransferase genes *UGT73B3* and *UGT73B5* is necessary for resistance to *Pseudomonas syringae* pv *tomato* in Arabidopsis. Plant Physiol **139:** 1890–1901

Lawton K, Weymann K, Friedrich L, Vernooij B, Uknes S, Ryals J (1995) Systemic acquired resistance in *Arabidopsis* requires salicylic acid but not ethylene. Mol Plant Microbe Interact **8:** 863–870

Lorrain S, Vailleau F, Balagué C, Roby D (2003) Lesion-mimic mutants: keys for deciphering cell death and defense pathways in plants. Trends Plant Sci **8:** 263–271

Martínez C, Pons E, Prats G, León J (2004) Salicylic acid regulates flowering time and links defence responses and reproductive development. Plant J **37:** 209–217

Mateo A, Mühlenbock P, Rustérucci C, Chi-Chen Chang C, Miszalski Z, Karpinska B, Parker JE, Mullineaux PM, Karpinski S (2004) *LESION SIMULATING DISEASE1* is required for acclimation to conditions that promote excess excitation energy. Plant Physiol **136:** 2818–2830

Meng PH, Raynaud C, Tcherkez G, Blanchet S, Massoud K, Domenichini S, Henry Y, Soubigou-Taconnat L, Lelarge-Trouverie C, Saindrenan P, et al (2009) Crosstalks between myo-inositol metabolism, programmed cell death and basal immunity in *Arabidopsis*. PLoS ONE **4:** e7364

Mittler R, Herr EH, Orvar BL, Van Camp W, Willekens H, Inzé D, Ellis BE (1999) Transgenic tobacco plants with reduced capability to detoxify reactive oxygen intermediates are hyperresponsive to pathogen infection. Proc Natl Acad Sci USA **96:** 14165–14170

Mittler R, Vanderauwera S, Gollery M, Van Breusegem F (2004) The reactive oxygen gene network in plants. Trends Plant Sci **9:** 490–498

Møller IM, Jensen PE, Hansson A (2007) Oxidative modifications to cellular components in plants. Annu Rev Plant Biol **58:** 459–481

Nafisi M, Goregaoker S, Botanga CJ, Glawischnig E, Olsen CE, Halkier BA, Glazebrook J (2007) *Arabidopsis* cytochrome P450 monooxygenase 71A13 catalyzes the conversion of indole-3-acetaldoxime in camalexin synthesis. Plant Cell **19:** 2039–2052

Narendra S, Venkataramani S, Shen G, Wang J, Pasapula V, Lin Y, Korneyev D, Holaday AS, Zhang H (2006) The *Arabidopsis* ascorbate peroxidase 3 is a peroxisomal membrane-bound antioxidant enzyme and is dispensable for *Arabidopsis* growth and development. J Exp Bot **57:** 3033–3042

Nawrath C, Métraux JP (1999) Salicylic acid induction-deficient mutants of *Arabidopsis* express *PR-2* and *PR-5* and accumulate high levels of camalexin after pathogen inoculation. Plant Cell **11:** 1393–1404

Nishizawa A, Yabuta Y, Shigeoka S (2008) Galactinol and raffinose constitute a novel function to protect plants from oxidative damage. Plant Physiol **147:** 1251–1263

Noctor G, Bergot G, Mauve C, Thominet D, Lelarge-Trouverie C, Prioul JL (2007) A comparative study of amino acid measurement in leaf extracts by gas chromatography-time of flight-mass spectrometry and high performance liquid chromatography with fluorescence detection. Metabolomics **3:** 161–174

Noctor G, Veljovic-Jovanovic S, Driscoll S, Novitskaya L, Foyer CH (2002) Drought and oxidative load in the leaves of C_3 plants: a predominant role for photorespiration? Ann Bot (Lond) **89:** 841–850

Nyathi Y, Baker A (2006) Plant peroxisomes as a source of signalling molecules. Biochim Biophys Acta **1763:** 1478–1495

Queval G, Hager J, Gakière B, Noctor G (2008) Why are literature data for H_2O_2 contents so variable? A discussion of potential difficulties in quantitative assays of leaf extracts. J Exp Bot **59:** 135–146

Queval G, Issakidis-Bourguet E, Hoeberichts FA, Vandorpe M, Gakière B, Vanacker H, Miginiac-Maslow M, Van Breusegem F, Noctor G (2007) Conditional oxidative stress responses in the Arabidopsis photorespiratory mutant *cat2* demonstrate that redox state is a key modulator of daylength-dependent gene expression, and define photoperiod as a crucial factor in the regulation of H_2O_2-induced cell death. Plant J **52:** 640–657

Queval G, Noctor G (2007) A plate reader method for the measurement of NAD, NADP, glutathione, and ascorbate in tissue extracts: application to redox profiling during *Arabidopsis* rosette development. Anal Biochem **363:** 58–69

Queval G, Thominet D, Vanacker H, Miginiac-Maslow M, Gakière B, Noctor G (2009) H_2O_2-activated up-regulation of glutathione in Arabidopsis involves induction of genes encoding enzymes involved in cysteine synthesis in the chloroplast. Mol Plant **2:** 344–356

Rizhsky L, Hallak-Herr E, Van Breusegem F, Rachmilevitch S, Barr J, Rodermel S, Inzé D, Mittler R (2002) Double antisense plants lacking ascorbate peroxidase and catalase are less sensitive to oxidative stress than single antisense plants lacking ascorbate peroxidase or catalase. Plant J **32:** 329–342

Sagi M, Fluhr R (2006) Production of reactive oxygen species by plant NADPH oxidases. Plant Physiol **141:** 336–340

Smith IK, Kendall AC, Keys AJ, Turner JC, Lea PJ (1984) Increased levels of glutathione in a catalase-deficient mutant of barley (*Hordeum vulgare* L.). Plant Sci Lett **37:** 29–33

Tada Y, Spoel SH, Pajerowska-Mukhtar K, Mou Z, Song J, Wang C, Zuo J, Dong X (2008) Plant immunity requires conformational changes of NPR1 via S-nitrosylation and thioredoxins. Science **321:** 952–956; erratum **Tada Y, Spoel SH, Pajerowska-Mukhtar K, Mou Z, Song J, Wang C, Zuo J, Dong X** (2008) Science **325:** 1072

Takahashi H, Chen Z, Du H, Liu Y, Klessig DF (1997) Development of necrosis and activation of disease resistance in transgenic tobacco plants with severely reduced catalase levels. Plant J **11:** 993–1005

Taler D, Galperin M, Benjamin I, Cohen Y, Kenigsbuch D (2004) Plant *eR* genes that encode photorespiratory enzymes confer resistance against disease. Plant Cell **16:** 172–184

Thomma BPHJ, Nelissen I, Eggermont K, Broekaert WF (1999) Deficiency in phytoalexin production causes enhanced susceptibility of *Arabidopsis thaliana* to the fungus *Alternaria brassicicola*. Plant J **19:** 163–171

Torres MA, Jones JDG, Dangl JL (2005) Pathogen-induced, NADPH oxidase-derived reactive oxygen intermediates suppress spread of cell death in *Arabidopsis thaliana*. Nat Genet **37:** 1130–1134

Torres MA, Jones JDG, Dangl JL (2006) Reactive oxygen species signaling in response to pathogens. Plant Physiol **141:** 373–378

Triantaphylidès C, Krischke M, Hoeberichts FA, Ksas B, Gresser G, Havaux M, Van Breusegem F, Mueller MJ (2008) Singlet oxygen is the major reactive oxygen species involved in photooxidative damage to plants. Plant Physiol **148:** 960–968

Van Breusegem F, Dat JF (2006) Reactive oxygen species in plant cell death. Plant Physiol **141:** 384–390

Vandenabeele S, Vanderauwera S, Vuylsteke M, Rombauts S, Langebartels C, Seidlitz HK, Zabeau M, Van Montagu M, Inzé D, Van Breusegem F (2004) Catalase deficiency drastically affects gene expression induced by high light in *Arabidopsis thaliana*. Plant J **39:** 45–58

Vanderauwera S, Zimmermann P, Rombauts S, Vandenabeele S, Langebartels C, Gruissem W, Inzé D, Van Breusegem F (2005) Genome-wide analysis of hydrogen peroxide-regulated gene expression in Arabidopsis reveals a high light-induced transcriptional cluster involved in anthocyanin biosynthesis. Plant Physiol **139:** 806–821

Van Wees SCM, Glazebrook J (2003) Loss of non-host resistance of *Arabidopsis NahG* to *Pseudomonas syringae* pv. *phaseolicola* is due to degradation products of salicylic acid. Plant J **33:** 733–742

Vlot AC, Dempsey DA, Klessig DF (2009) Salicylic acid, a multifaceted hormone to combat disease. Annu Rev Phytopathol **47:** 177–206

Volk S, Feierabend J (1989) Photoinactivation of catalase at low temperature and its relevance to photosynthetic and peroxide metabolism in leaves. Plant Cell Environ **12:** 701–712

Vollsnes AV, Erikson AB, Otterholt E, Kvaal K, Oxaal U, Futsaether C (2009) Visible foliar injury and infrared imaging show that daylength affects short-term recovery after ozone stress in *Trifolium subterraneum*. J Exp Bot **60:** 3677–3686

Vuylsteke M, Peleman JD, van Eijk MJT (2007) AFLP-based transcript profiling (cDNA-AFLP) for genome-wide expression analysis. Nat Protoc **2:** 1399–1413

Wagner D, Przybyla D, Op den Camp R, Kim C, Landgraf F, Lee KP, Würsch M, Laloi C, Nater M, Hideg E, et al (2004) The genetic basis of singlet oxygen-induced stress responses of *Arabidopsis thaliana*. Science **306:** 1183–1185

Wäspi U, Schweizer P, Dudler R (2001) Syringolin reprograms wheat to undergo hypersensitive cell death in a compatible interaction with powdery mildew. Plant Cell **13:** 153–161

Wildermuth MC, Dewdney J, Wu G, Ausubel FM (2001) Isochorismate synthase is required to synthesize salicylic acid for plant defence. Nature **414:** 562–565; erratum **Wildermuth MC, Dewdney J, Wu G, Ausubel FM** (2001) Nature **417:** 571

Willekens H, Chamnongpol S, Davey M, Schraudner M, Langebartels C, Van Montagu M, Inzé D, Van Camp W (1997) Catalase is a sink for H_2O_2 and is indispensable for stress defence in C_3 plants. EMBO J **16:** 4806–4816

Yu L, Wan F, Dutta S, Welsh S, Liu Z, Freundt E, Baehrecke EH, Lenardo M (2006) Autophagic programmed cell death by selective catalase degradation. Proc Natl Acad Sci USA **103:** 4952–4957

Zhao J, Last RL (1996) Coordinate regulation of the tryptophan biosynthetic pathway and indolic phytoalexin accumulation in *Arabidopsis*. Plant Cell **8:** 2235–2244

Zhou N, Tootle TL, Tsui F, Klessig DF, Glazebrook J (1998) *PAD4* functions upstream from salicylic acid to control defense responses in *Arabidopsis*. Plant Cell **10:** 1021–1030